HSV-1 strains circulating in Finland demonstrate uncoupling of geographic and phenotypic variation

[1]Christopher D. Bowen, [2#]Henrik Paavilainen, [1#]Daniel W. Renner, [2]Jussi Palomäki, [2]Jenni Lehtinen, [3]Tytti Vuorinen, [4]Peter Norberg, [2*]Veijo Hukkanen, [1*]Moriah L. Szpara

[1]Department of Biochemistry and Molecular Biology, Center for Infectious Disease Dynamics, and the Huck Institutes of the Life Sciences, Pennsylvania State University, University Park, Pennsylvania 16802, USA
[2] Institute of Biomedicine, University of Turku, Kiinamyllynkatu 10 D, FIN-20520 Turku, Finland
[3]Clinical Microbiology, Turku University Hospital and Institute of Biomedicine, University of Turku, Kiinamyllynkatu 13, FIN-20520 Turku, Finland
[4]Department of Virology, University of Gothenburg, Gothenburg, Sweden

#equal contribution of DWR and HP
***equal contribution of MLS and VH**

Corresponding Author:
Moriah L. Szpara
Dept. of Biochemistry & Molecular Biology
The Huck Institutes of the Life Sciences
W-208 Millennium Science Complex (MSC)
Pennsylvania State University
University Park, PA 16802 USA
Phone: 814-867-0008
Email: moriah@psu.edu

Author emails:
Christopher D. Bowen: cdb5004@psu.edu
Henrik Paavilainen: hojpaa@utu.fi
Daniel W. Renner: dwr19@psu.edu
Jussi Palomäki: jmmpal@utu.fi
Jenni Lehtinen: jen_ni_90@hotmail.com
Tytti Vuorinen: tyvuori@utu.fi
Peter Norberg: peter.norberg@microbio.gu.se
Veijo Hukkanen: veijo.hukkanen@utu.fi
Moriah L. Szpara: moriah@psu.edu

Abstract

A majority of adults in Finland are seropositive carriers of herpes simplex viruses (HSV). Infection occurs at epithelial or mucosal surfaces, after which virions enter innervating nerve endings, eventually establishing lifelong infection in neurons of the sensory or autonomic nervous system. Recent data have highlighted the genetic diversity of HSV-1 strains, and demonstrated apparent geographic patterns in strain similarity. Though multiple HSV-1 genomes have been sequenced from Europe to date, there is a dearth of sequenced genomes from Nordic countries. Finland's history includes at least two major waves of human migration, suggesting the potential for diverse viruses to persist in the population. Here we used HSV-1 clinical isolates from Finland to test the relationship between viral phylogeny, genetic variation, and phenotypic characteristics. We found that Finnish HSV-1 isolates separated into two distinct phylogenetic groups, potentially reflecting the two historical waves of human (and viral) migration into Finland. The amount of genetic diversity found in these ten clinical isolates was similar to that found between independent HSV-1 strains from other geographic areas. These HSV-1 isolates harbored distinct phenotypes in cell culture, including differences in virus production, extracellular virus release, and cell-type-specific fitness. Importantly, these phenotypic differences did not partition into the same groups as the phylogenetic clusters, demonstrating that whole-genome relatedness is not a proxy for overall viral phenotype. Instead, we highlight specific gene-level differences that may contribute to observed phenotypic differences, and we note that strains from different phylogenetic groups contain the same genetic variations.

Keywords: Herpes simplex virus (HSV), comparative genomics, phylogeny, genotype, phenotype, genetic variation

63 # Introduction

64 Human herpes simplex virus 1 (HSV-1; Family: *Herpesviridae,* Genus: *Simplexvirus,* species:
65 *Human herpesvirus 1*) has been recognized as a major human malady since the era of
66 Hippocrates (1), and to this day there is no effective vaccine (2). Approximately 50% of adults in
67 Finland are seropositive for HSV-1 (3–5), and 13% are seropositive for HSV-2 (3, 6). HSV
68 infects via epithelial or mucosal surfaces, after which it is taken up by nerve endings and
69 establishes a lifelong infection in neurons of the sensory or sympathetic nervous system. From
70 these neuronal sites the virus can reactivate, transit via nerve endings back to the skin surface,
71 and re-initiate skin or mucosal shedding at the same site as the original infection. In addition to
72 recurrent epithelial lesions, HSV also causes infectious keratitis, worsens acquisition and
73 shedding rates for human immunodeficiency virus (HIV), and can progress to cause rare but life-
74 threatening encephalitis (1).

75 Recent comparative genomics studies of HSV-1, from our lab and others, have demonstrated that
76 HSV-1 strains from unrelated individuals can differ in 2-4% of the viral genome (7–13). HSV-1
77 has a large DNA genome of ~152 kilobases, encoding >75 proteins (14, 15). Sequence-based
78 comparisons of HSV-1 strains have demonstrated at least three major clades (16, 17), with
79 evidence of geographic clustering (9, 18), as well as recombination between these groups. HSV-
80 1 displays greater host-to-host variation than any other alpha-herpesvirus (9, 19): approximately
81 double the amount found in HSV-2 (20, 21), and 5-fold higher than found between isolates of
82 varicella zoster virus (VZV) (22–24). The impacts of these naturally occurring viral genetic
83 variations on virulence and pathogenesis in humans are unknown. Examining the phenotypic
84 differences displayed by HSV-1 strains in culture provides an opportunity to explore the scope of

85 these differences and test whether or not they are linked to previously observed patterns of
86 geographic diversity.

87 Finland has a unique history that has led to a relatively homogeneous and stable population,
88 providing a unique view on the evolution of viruses that are persistent in the population. There
89 have been two major migratory sweeps contributing to expansion of the human population of
90 Finland: the first wave from the east, occurring ca. 4000 years ago, and another wave from the
91 south (southwest) ca. 2000 years ago (25–27). Finland also has one of the best genealogical
92 databases in the world, which in combination with computerized medical records and a high rate
93 of patient participation, has led to many recent advances in human medical genetics (28, 29).
94 This may enable future studies to explore the co-evolution of human and viral genetic variation
95 in this population.

96 We have characterized ten HSV-1 strains isolated from a random subset of Finland clinic visits,
97 and compared their growth properties, drug resistance, and other phenotypic features. Full
98 genome sequences of these viruses were compared to each other and to other previously
99 described strains of HSV-1, to reveal patterns of inter-host and intra-host variability. We found
100 that the observed phenotypic differences did not partition into the same sub-groups as the overall
101 genomic patterns, demonstrating that whole-genome relatedness is not a proxy for viral
102 phenotype. We anticipate that these data will aid in efforts to develop improved sequence-based
103 antiviral therapies and contribute to development of a vaccine against HSV infections (30).
104 These data present an opportunity to explore the diversity of chronic herpesviruses in the Finland
105 population, and to lay the foundation for future studies that explore the connections between

106 viral genetic differences, host genetic predispositions, and their potential relationship(s) to
107 clinical outcomes of HSV-1 infection.

108

109 Methods

110 Virus isolates and virus stock propagation

111 Clinical isolates were obtained from anonymous coded diagnostic samples from herpes lesions
112 representing currently circulating viral strains in Finland (**Table 1**). Approval for the study of
113 anonymous HSV isolates was provided by the Turku University Central Hospital (permit #
114 J10/17).

115 An immunoperoxidase-rapid culture assay (31) was used to type the viruses as HSV-1, which
116 was confirmed by a HSV type-specific gD (US6) gene-based PCR test (32). Viruses were
117 initially propagated on Vero cells (African green monkey kidney cells; ATCC), maintained in
118 Dulbecco's MEM with 2% fetal calf serum and gentamycin. A stock was made by addition of 3
119 ml of 9% autoclaved skimmed milk (Valio, Finland) on to 5 ml of the culture medium and
120 subsequent freezing. The cells and the medium were collected and combined upon thawing, and
121 were frozen and thawed for two further rounds before aliquoting. The viral titer was determined
122 by plaque titration on Vero cells as described before (33). Parallel aliquots were used for further
123 viral culture studies and for preparation of viral nucleocapsid DNA. For viral production data,
124 SPSS Statistics 20 (IBM, Armonk NY, USA) software was use to perform statistical analyses.
125 Non-parametric Mann-Whitney U-test was used to calculate statistical significances. The
126 threshold for significance was set to $p<0.05$.

127 **Viral genomic DNA isolation**

128 The viral genomic DNA was prepared from isolated viral nucleocapsids as described previously
129 (7, 34). In brief, viral stock collected from the first or second passage in Vero cells was used to
130 infect ~$1x10^8$ HaCaT cells (Department of Dentistry, University of Turku (35)) at a multiplicity
131 of infection (m.o.i.) of 0.1-1 plaque-forming units (PFU)/cell, and the infection was allowed to
132 proceed to completion at +35 °C (1-3 days). The cells were collected, washed with PBS and
133 suspended to LCM buffer (0.125 M KCl, 30 mM Tris pH 7.4, 5 mM $MgCl_2$, 0.5 mM EDTA,
134 0.5% Nonidet P-40; with 0.6 mM beta-mercaptoethanol). After two successive extractions with
135 Freon (1,1,2-trichloro-1,2,2-trifluoroethane, Sigma-Aldrich), the extracts were added on top of
136 layers in LCM buffer with 45% and 5% glycerol and ultracentrifuged at 77 000 x g for 1 h at
137 +4ºC (Beckman Coulter SW41Ti rotor). Viral nucleocapsids were recovered from the bottom of
138 the ultracentrifuge tube, and the DNA was prepared by treatment with Proteinase K and SDS,
139 followed by repeated extractions with phenol-chloroform and ethanol precipitation. The DNA
140 content and purity were observed by spectrophotometry and by agarose gel electrophoresis after
141 restriction enzyme digestions.

142 **Cell culture**

143 Vero cells (ATCC; Manassas, VA) were propagated in M199 medium supplemented with 5%
144 fetal bovine serum and gentamycin. HaCaT cells (Department of Dentistry, University of Turku;
145 (35)) were propagated in DMEM medium with HEPES buffer, supplemented with 7% fetal
146 bovine serum and gentamycin. SH-SY5Y neuroblastoma cells (K. Åkerman, Åbo Akademi
147 University, Turku, Finland) were propagated in DMEM (high glucose) medium supplemented
148 with 10% fetal bovine serum, 2 mM L-glutamine and gentamycin. Initial differentiation of SH-

149 SY5Y cells involved culture for 10 days in DMEM/F-12 medium containing 5% fetal bovine
150 serum, 10 μM All-trans retinoic acid (Sigma), 2 mM L-glutamine and gentamycin. Thereafter
151 SH-SY5Y cells were transferred on Matrigel-coated (B-D) 96-well plates and the medium was
152 changed to serum-free DMEM/F-12 medium containing 10 μM all-trans retinoic acid (Sigma),
153 0.5 μg/ml of brain-derived neurotrophic factor (Millipore), 2 mM L-glutamine and gentamycin.

154 **Acyclovir resistance testing**

155 The sensitivity of each HSV strain to acyclovir was tested in a microplate format. Vero cells
156 grown on 96-well cell culture plates were treated with cell culture medium (DMEM with 5%
157 fetal bovine serum) supplemented with acyclovir (ACV; Sigma), in concentrations of 128 μg/ml
158 to 0.03125 μg/ml (1:4 serial dilutions). Duplicate wells containing each ACV dilution, and wells
159 without ACV, were infected with 100 PFU of each virus. As a control, the HSV-1 delta305 virus
160 was included; it is resistant to ACV due to deletion of its thymidine kinase gene (36). Infected
161 cells were incubated at +37°C, at 5% CO_2, for 72 hours before fixation with methanol and
162 staining with crystal violet. The reduction of plaque numbers at each ACV dilution was observed
163 in comparison with wells infected without ACV. A logistic fit curve was used for determination
164 of IC_{50} values. A virus with an IC_{50} value of over 2 μg/ml (of ACV) was considered resistant
165 (37).

166 **Image acquisition**

167 Photomicrographic images of viral plaques were obtained using a Zeiss Primovert inverted
168 microscope with Plan-Achromat 4x and 10x objectives, recorded using an AxioCam ERc 5s
169 camera, and analyzed using Zeiss ZEN 2012 software.

170 **Next generation sequencing**

171 Viral nucleocapsid DNA was sheared on a Covaris M220 (parameters: 60 seconds duration, peak
172 power 50, 10% duty cycle, 4C). We used the Illumina TruSeq DNA Sample Prep kit to prepare
173 barcoded sequencing libraries, according to the manufacturer's protocol for low-throughput
174 sample handling. Libraries were quantified and assessed by Qubit (Invitrogen, CA), Bioanalyzer
175 (Agilent), and library adapter qPCR (KAPA Biosystems). Illumina MiSeq paired-end sequencing
176 (2 x 300 bp) was completed according to manufacturer's recommendations, using 17 pM library
177 concentration.

178 A consensus viral genome for each strain was assembled using a *de novo* viral genome assembly
179 (VirGA) workflow (10). This approach begins with quality control, including removal of
180 contaminating host sequences, adapters from library preparation, and imaging artifacts. Next
181 VirGA iterates through multiple *de novo* assemblies using SSAKE, which we then combine into
182 longer blocks of sequence (contigs) using Celera and GapFiller. VirGA uses Mugsy alignment to
183 match these contigs to the HSV-1 reference genome (strain 17, GenBank accession JN555585).
184 The best-matched contigs are stitched into a single consensus genome, which is then annotated
185 and subjected to additional quality control measures. These include an examination of coverage
186 (sequence read) depth, detection of minority variants within each consensus genome, and manual
187 inspection of gaps and low coverage areas. See **Table 2** for GenBank accessions.

188 **Intra-strain minority-variant detection**

189 Minority-variant (MV) positions within each *de novo* assembled genome were determined using
190 VarScan v2.2.11 as previously described (38, 39). Conservative variant calling parameters to

191 eliminate sequencing-induced errors were set at: minimum allele frequency ≥0.02; base call
192 quality ≥20; read depth at the position ≥100; independent reads supporting minor allele ≥5. MVs
193 containing ≥90% unidirectional strand support were excluded from further analyses (40, 41).
194 MVs passing quality control were mapped to respective genomes and assessed for mutational
195 effect using SnpEff and SnpSift (42, 43).

196 **Phylogenetic and recombination analyses**

197 DNA sequences were aligned using the Kalign algorithm included in eBioTools. To avoid
198 inferences caused by false phylogenetic signals, all gap and repeat regions were excluded prior to
199 this analysis. Repeat regions not leading to gaps were also excluded since these may contain
200 single nucleotide differences that have been shuffled into new positions by random aspects of
201 tandem-repeat alignment. Furthermore, ambiguous nucleotides that were marked as "N" were
202 excluded, along with the corresponding aligned nucleotides in remaining sequences. Complete
203 genomes in GenBank harbouring long stretches of "N" were not included in the analysis (e.g.
204 strain B3x_1_5). In total, 110,168 nucleotides were analysed in each genome.

205 The phylogenetic network was constructed by using SplitsTree4. It is a NeighborNet with
206 OrdinaryLeastSquares Variance depicted as a RootedEqualAngle splits tree. A recombination
207 test on the complete dataset was performed by using the Phi test for recombination implemented
208 in SplitsTree4.

209 **Restriction fragment length polymorphism (RFLP) analysis**

210 A cytoplasmic viral DNA preparation was modified from the protocol described by Igarashi et al
211 (44). Subconfluent Vero cell cultures were infected at an m.o.i of 0.1, and incubated at +34°C for

212 2 days until the cytopathic effect was complete. The cells were collected in 150 mM NaCl, 10
213 mM Tris pH 7.6, 1.5 mM MgCl buffer, with 0.1% Nonidet P-40. The nuclei were pelleted, and
214 DNA was extracted from the supernatant by two successive extractions with phenol-chloroform.
215 DNA was recovered by ethanol precipitation. 12.5 µg of each viral DNA was diluted in 15 µl
216 solution containing sterile H_2O, FastDigest 10X green buffer and FastDigest BamHI or SalI
217 restriction enzyme (Thermo Scientific). Electrophoresis was run in 0.8 % TBE-agarose gels, with
218 GeneRuler mix DNA ladder, for 24 h at 45 V before imaging. In order to separate large DNA
219 fragments after SalI digestion, electrophoresis was continued for additional 36 h at 30 V.

220

221 # Results

222 ## Comparison of growth properties of Finnish HSV-1 strains in vitro

223 A random set of ten circulating Finnish HSV-1 isolates were selected from residual laboratory
224 diagnostic specimens (**Table 1)**. We first examined *in vitro* phenotypic characteristics of these
225 HSV-1 isolates, by comparing their overall titer and rate of intracellular virus vs. extracellular
226 (released) virus production at 24 hours post infection (hpi) of a range of cell types (**Figure 1**).
227 These included non-human primate kidney-derived epithelial (Vero) cells (**Figure 1A**), human
228 keratinocyte (HaCaT) cells (**Figure 1B**), and human neuroblastoma (SH-SY5Y) cells in a mixed,
229 undifferentiated state (**Figure 1C**), as well as a differentiated, neuronal state (**Figure 1D**).
230 Compared to epithelial and keratinocyte cells, overall viral production was markedly reduced in
231 neuronal precursor cells and differentiated neuronal cells (compare **Figure 1AB** vs. **CD**). The
232 wild-type HSV-1 reference strain 17+ replicated to significantly higher titers than any of the

233 circulating clinical isolates in Vero cells, which are standardly used for HSV propagation, and to
234 a lesser extent strain 17+ replicated at higher titer in other cell types as well (**Figure 1**; $p<0.05$,
235 10-100 fold higher viral amounts). Different clinical isolates excelled at producing virions in
236 each cell type, with no clear patterns of most- or least-efficient viral production or release across
237 all cell types. The amount of extracellular released virus was less than 10% of the total virion
238 production, in all cell types except the undifferentiated neuronal precursor cells (**Supplemental**
239 **Figure S1**). Each virus strain was also tested for acyclovir (ACV) resistance. Despite some
240 variation in ACV susceptibility (IC50 values), none of the circulating Finnish viruses was
241 considered resistant to ACV (**Table 1**). There were also no significant differences among the 10
242 clinical isolates in the plaque morphology or the type of cytopathic effect induced in Vero cell
243 cultures (**Figure 2**).

244 Genetic and genomic analysis of Finnish HSV-1 strains

245 Based on prior data suggesting the effects of successive waves of migration on the human
246 population in Finland (25, 26), we next assessed the overall genetic diversity of these ten HSV-1
247 isolates. We first performed a restriction fragment length polymorphism (RFLP) analysis on viral
248 genomic DNA, which revealed at least two broad patterns of variation (**Figure 3** and
249 **Supplemental Figure S2**). The diversity of bands led us to examine these genetic differences
250 with greater precision using high-throughput, deep genome sequencing (HTS) and comparative
251 genomics analysis (see **Methods** for details). A previously described bioinformatics pipeline was
252 used to *de novo* assemble a full-length consensus genome for each strain **(Table 2)**. A viral
253 consensus genome represents the most common nucleotide detected at each nucleotide position
254 in that viral population. All viral genomes had a coverage depth between 1,000-2,800-fold, with

255 >96% of the genome covered at a depth exceeding 100-fold **(Table 2)**. This depth enabled us to
256 compare the full genetic complement of the viral genome for each strain, and to analyze
257 differences both between and within each viral strain population, and to compare them to
258 previously described viral genomes.

259 Genetic relatedness of Finland HSV-1 samples

260 First, we used the viral consensus genomes to compare how overall variation in these ten Finnish
261 HSV-1 genomes related to the patterns observed by RFLP analysis (**Figure 3**). Whole genome
262 alignments were created using the ten Finnish HSV-1 genomes, as well as these ten in
263 conjunction with a diverse set of previously published HSV-1 genomes (see Methods and
264 **Supplemental Table S1** for a full list). We then used SplitsTree to create a network graph that
265 revealed the relatedness of the ten Finnish viral genomes to each other (**Figure 4A**) and to
266 previously described HSV-1 genomes (**Figure 4B**). This approach revealed that the Finland
267 HSV-1 genomes separated into two sub-groups, which appear to relate to previously recognized
268 Asian and European / North American clades. These data echo those of the initial RFLP analysis.

269 Protein-coding variation in Finland HSV-1 samples

270 Next, we examined more fine-scale genetic differences in these HSV-1 isolates, which are
271 invisible at the level of RFLP analysis. Here we examined DNA- and amino acid (AA)-
272 alignments for each protein-coding region of the HSV-1 genome (**Supplemental Table S2-S3**).
273 We found that from zero to 8% of each coding region differed at the AA level between the ten
274 Finnish viral genomes (**Figure 5**). Only a handful of small coding regions (UL20, VP26 (UL35),
275 UL49A, UL55) showed no AA variation at all between viral isolates. Consistent with previous

276 findings (9), gL (UL1), UL11, UL43, gG (US4), and gJ (US5) were among the most divergent
277 proteins. Together these inter-strain genetic differences in 70 HSV-1 proteins in **Figure 5**
278 provide ample opportunities to generate the phenotypic diversity observed in **Figure 1**. Overall,
279 these levels of AA coding diversity reflect those seen in previous analyses (9), and between other
280 known HSV-1 genomes.

281 **Minority allelic variants in Finland HSV-1 viral populations**

282 Each viral consensus genome represents the most common nucleotide detected at each position
283 in the viral genome. In contrast, minority variants (MV) within each viral population are rare
284 alleles, presented in <50% of the sequenced reads. These MV may rise to greater prevalence
285 during viral spread to new niches or hosts, or under selective evolutionary pressure. For each
286 viral genome, we examined the number of MVs detected in each genome. Stringent quality-
287 control criteria were used to reduce the number of false-positive MVs (see **Methods**), such that
288 only those MV detected at ≥2% prevalence were used in this analysis. MVs were found
289 dispersed across each genome (**Supplemental Figure S3**), mostly in intergenic regions. A
290 concentration of MVs were found near tandem repeats in VP1/2 (UL36), gI (US7), and in the
291 internal-repeat regions, which may result from stochasticity in tandem repeat alignment in these
292 regions. The MVs detected in gI occur at the same tandem-repeat site as the consensus-level AA
293 variations in this gene (**Figure 6**). Taken together, these results define the level of inter-host
294 (**Figure 5**) and intra-host (**Supplemental Figure S3**) variation seen in the Finnish HSV-1 strains
295 described herein.

296 **Patterns of variation in Finnish HSV-1 strains**

297 Finally, we considered whether any of the observed patterns of genomic or phenotypic variation
298 could be linked to fine-scale coding variations in these ten Finnish HSV-1 isolates. The genomic
299 sub-groups detected by RFLP (**Figure 3**) and network graph analysis (**Figure 4**) were reflected
300 in several coding variations that correlated with phylogenetic group. For example, coding
301 differences in the secreted and virion surface glycoprotein G (gG; US4) correlated with the two
302 Finnish phylogenetic sub-groups (**Figure 6A**; see **Figure 4** for phylogenetic sub-groups). Other
303 impacts on coding variation may result from changes in copy number at tandem repeats.
304 Variation in tandem repeat length in glycoprotein I (gI; US7) leads to changes in the length of a
305 repeating tract of mucin-type O-linked glycosylation sites (**Figure 6B)**, akin to that previously
306 described in clinical isolates of HSV-1 (16, 45). Finally, there are detectable patterns of AA
307 variation that correlate with phenotypic differences in viral fitness in specific cell types. Coding
308 differences in the nuclear egress complex protein NEC2 (UL34) (**Figure 6C**) were observed in
309 the two strains (F-12g, M-15) which showed no detectable extracellular virion release in
310 differentiated neuronal cells (**Figure 1D**). The terminally differentiated and non-dividing state of
311 these neuronal cells may constitute a sensitized background to detect impacts on virion egress.
312 Taken together, these examples illustrate the type and degree of variation present in these strains,
313 and highlight potential genetic insights into viral phenotype.

314

315 # Discussion

316 In this study, we described the first-ever HSV-1 genomes from Finland. Two distinct sub-groups
317 or clades were observed in the ten Finnish clinical isolates, with four strains clustering in one
318 clade and six in another. These groups were detectable using both classical RFLP approaches
319 (**Figure 3**) and deep-sequencing methods for whole-genome analyses (**Figure 4**). These data
320 appear to corroborate previous findings that show multiple colonization events of Finland, with
321 migration from Europe in the south and Asia in the northeast (25, 26). However, we found that
322 phenotypic differences between these isolates were uncoupled from the overall genomic patterns
323 that grouped them into two geographic clades. While plaque morphology was consistent across
324 isolates (**Figure 2**), the amount of virus production, extracellular virion release, and acyclovir
325 sensitivity differed between isolates and across cell types (**Figure 1** and **Table 1**). We detected
326 gene-specific patterns of genetic variation that may well impact protein function. Future studies
327 will need to dissect individual genetic variations in each viral isolate in order to test their precise
328 impact(s) on viral fitness.

329 When analyzing the replication capabilities of these recently isolated clinical samples in multiple
330 cell types, we found that they replicated to lower overall titers and produced fewer extracellular
331 virions than the lab-adapted HSV-1 strain 17+, regardless of cell type (**Figure 1** and
332 **Supplemental Figure S1**). This difference was more pronounced in non-human primate and
333 human epithelial cells, and was more subtle in neuronal precursors and differentiated neuronal
334 cells. There did not appear to be any clear differences in titer or extracellular virus production
335 between geographic clades. There also seemed to be no noticeable differences in plaque
336 morphology among these samples, with plaque size and cellular cytopathic effect being similar

337 across all samples. Although we report findings in a number of cell lines in this study, it will be
338 important for future studies to examine each virus and cell-type pairing separately, since these
339 data demonstrate that maximal viral fitness in one cell type is not generally predictive of fitness
340 in another.

341 We observed several potential connections between genetic differences and phenotypic
342 differences. For instance, we detected an AA difference in the UL34 (NEC2) binding domain in
343 F-12g and M-15 **(Figure 6C).** Previous work has shown that the viral proteins UL31 (NEC1) and
344 UL34 (NEC2) form a nuclear egress complex that localizes to the perinuclear space and plays a
345 critical role in egress of viral capsids from the nucleus (46, 47). In these two clinical isolates (F-
346 12g and M-15), there was no measurable amount of extracellular virus produced in differentiated
347 neuronal cells (**Figure 1D**). Further studies will be needed to examine if this phenotype is linked
348 to a disruption of NEC1 and NEC2 binding and impaired nuclear egress for isolates F-12g and
349 M-15. Variation in the copy-number of tandem repeats is yet another way that HSV-1 isolates
350 can generate genetic and potential phenotypic variation. Glycoprotein I (gI; US7) contains a
351 mucin-like domain with repeating units of serine, threonine, and proline (**Figure 6B**). This
352 domain varies in length across these isolates. This domain has been previously shown to serve as
353 a site of O-linked glycosylation, with longer tracts (e.g. 8 repeating blocks of 7 AA each) being
354 more heavily glycosylated than short tracts (e.g. 2 repeating blocks) (16, 45). A prior study of
355 over 80 Swedish HSV-1 isolates found roughly equal distributions of isolates with two, three, or
356 four repeating blocks in this mucin-like gI domain (16, 45). Half of the Finland HSV-1 isolates
357 analyzed here have at least four repeating units, suggesting the potential for gI to be more

358 heavily glycosylated in these isolates. These data generate hypotheses for future investigations of
359 genotype-phenotype links in these and other new clinical isolates.

360 This study provides one of the first combinations of phenotypic analyses that span multiple cell
361 types, alongside full comparative genomic analyses that span both phylogenetic and gene-
362 specific analyses. One comparison not yet explored in this or prior studies is the specific pairing
363 of each virus with cells derived from the human source of each isolate. This approach is now
364 technically feasible, using induced pluripotent stem cell technology to generate specific cell
365 types from a single source such as a buccal swab. The rich genealogical databases in Finland
366 suggest an opportunity to not only pair these analyses at the human-cell and virus level, but also
367 to link observed phenotypes of cellular infection to each patient's clinical and/or familial history
368 of herpesvirus disease. We anticipate that in the future, this approach would yield fruitful
369 insights not only into direct clinical outcomes of herpesvirus disease, but also generate
370 hypotheses about herpesvirus co-morbidities.

371

372 **Acknowledgements**

373 The authors thank members of the Hukkanen and Szpara labs for helpful feedback and
374 discussion. We acknowledge Ritva Kajander for preparation of the viral stocks and the viral
375 nucleocapsid DNA. This work was supported by research startup funds (MLS) from the
376 Pennsylvania State University, and by a grant from the Pennsylvania Department of Health using
377 CURE funds (MLS). The Department specifically disclaims responsibility for any analyses,
378 interpretations, or conclusions. The funding from the Jane and Aatos Erkko Foundation grant

379 #170046 is acknowledged. We thank Prof. Bernard Roizman, University of Chicago, for the
380 delta305 virus.

381 Figure Legends

382 **Figure 1: Comparison of growth properties of Finnish HSV-1 strains reveals the**
383 **uncoupling of phenotypic and geographic variation.**

384 Histograms comparing virus production for ten Finnish strains of HSV-1, as compared to the
385 HSV-1 reference strain 17+, in different cell types. Panel **(A,** non-human primate**)** shows Vero
386 monkey kidney cells, which are defective in interferon signaling; **(B)** shows HaCaT human
387 epithelial cells; **(C)** shows undifferentiated human SH-SY5Y neuroblastoma cells (neuronal
388 precursor cells); **(D)** shows differentiated human SH-SY5Y neuronal-like cells. Viruses are
389 plotted in descending order based on their viral production, and divided into their genomic sub-
390 groups (see **Figure 4**). Each histogram bar plots infectious virions in the cell-associated fraction
391 (gray) vs. those released from cells (black). **Supplemental Figure S1** shows the same data, but
392 with extracellular released virus plotted as a percentage of total virus production. Bar shows
393 SEM; * = p=<0.05, ** = p<0.001 as compared to the total virus amount (cell associated + shed),
394 clinical isolate vs HSV-1(17+) reference strain.

395 **Figure 2. Finnish HSV-1 strains have similar plaque morphology.**

396 Typical morphology of the plaques of the clinical HSV-1 isolates on Vero cells, at 48 hours post
397 infection. Plaques are shown at low magnification (4X, **A,C**), as well as high magnification
398 (10X, **B,D**). Isolates M-19 (**A-B**) and F-12g (**C,D**) serve as representative examples. These two
399 isolates also represent the two sub-groups of Finnish HSV-1 isolates detected in **Figures 3-4**, as

400 well as samples annotated as blister-derived (M-19) and genital-blister-derived (F-12g) (see also
401 **Table 1**). The scale bar corresponds to 100 μm in panels A and C, and to 50 μm in panels B and
402 D.

403 **Figure 3: RFLP comparison reveals at least two sub-groups of Finnish HSV-1**
404 **strains.**

405 Viral genomic DNA was digested with SalI and separated via electrophoresis to distinguish
406 overall genetic patterns. Classically defined SalI fragment notations (red alphabet letters) are
407 indicated on the left (48). Predicted SalI cut-sites in each viral genome are shown in
408 **Supplemental Figure S2**. Red crosses (x) indicate variation in the size of SalI fragment G, while
409 diamonds indicate variation in the SalI Q fragment.

410 **Figure 4. A network graph of genetic relatedness reveals that Finland HSV-1**
411 **isolates separate into two sub-groups.**

412 A network graph of genetic relatedness was constructed using SplitsTree4 to demonstrate how
413 the ten new Finland HSV-1 isolates relate to each other (**A**) and to previously described HSV-1
414 genomes from a diversity of locations (**B**). Geographic clustering of branches and clades
415 resemble those previously described (9, 16–18) and are colored by origin of strains: red for
416 Europe and North America, blue for Asia, and purple for Africa. Finland HSV-1 genomes are
417 indicated in bold, and separate into two sub-groups (**A**), which appear to relate previously
418 recognized Asian and European and North American clades. The isolate name, country of origin,
419 GenBank accession, and reference(s) for each previously described HSV-1 genome are listed in
420 **Supplemental Table S1**.

421 **Figure 5. Substantial protein-coding variation exists between Finland HSV-1**
422 **isolates.**
423 Histogram showing each protein of the HSV-1 genome and its percent amino acid (AA) variation
424 between the ten Finnish HSV-1 strains compared here. Labels for the Unique Long (UL) and
425 Unique Short (US) regions of the HSV-1 genome are shown in summary format, to the left of
426 each sequentially-numbered viral coding region. Where possible, the common name of each
427 protein is shown to the right of the appropriate histogram bar, e.g. UL1 is also known as gL. AA
428 differences were quantified at the consensus level of each viral genome. See **Supplemental**
429 **Table S2** for additional data on the number of nucleotide differences and dN/dS ratio for each
430 gene.

431 **Figure 6. Patterns of genetic variation in Finnish HSV-1 strains correlate with**
432 **genomic and phenotypic data.**
433 Diagrams depict three HSV-1 proteins with known functional domains and post-translational
434 modifications (e.g. phosphorylation, glycosylation; see Legend). A subset of each protein is
435 highlighted via an AA alignment of the ten clinical HSV-1 isolates. (**A**) Coding differences in the
436 secreted and virion surface glycoprotein G (gG; US4) correlate with the overall genomic sub-
437 groups (clades) shown in **Figure 4**. (**B**) Variation in copy number of a seven AA tandem repeat
438 block in glycoprotein I (gI; US7) changes the length of a repeating tract of mucin-type O-linked
439 glycosylation sites, as described previously in clinical isolates of HSV-1 (16, 45). (**C**) AA
440 differences in the nuclear egress protein NEC2 (UL34) were observed in the two strains (M-15,
441 F-12g) which showed no detectable extracellular virion release in differentiated neuronal cells
442 (**Figure 1D**).

443 # References

444 1. Roizman B, Sears E. 1996. Herpes simplex viruses and their replication, p. 1043–1107. *In*
445 Fields, BN, Knipe, DM, Howley, PM (eds.), Fundamental virology, 3rd ed. Lippincott-
446 Raven, Philadelphia, PA.

447 2. Johnston C, Koelle DM, Wald A. 2011. HSV-2 : in pursuit of a vaccine. J Clin Invest
448 121:4600–4609.

449 3. Pebody RG. 2004. The seroepidemiology of herpes simplex virus type 1 and 2 in Europe.
450 Sex Transm Infect 80:185–191.

451 4. Puhakka L, Sarvikivi E, Lappalainen M, Surcel H-M, Saxen H. 2016. Decrease in
452 seroprevalence for herpesviruses among pregnant women in Finland: cross-sectional study
453 of three time points 1992, 2002 and 2012. Infect Dis 48:406–410.

454 5. Looker KJ, Magaret AS, May MT, Turner KME, Vickerman P, Gottlieb SL, Newman LM.
455 2015. Global and regional estimates of prevalent and incident herpes simplex virus type 1
456 infections in 2012. PLoS ONE 10:e0140765.

457 6. Looker KJ, Magaret AS, Turner KME, Vickerman P, Gottlieb SL, Newman LM. 2015.
458 Global estimates of prevalent and incident herpes simplex virus type 2 infections in 2012.
459 PloS One 10:e114989.

460 7. Szpara ML, Parsons L, Enquist LW. 2010. Sequence variability in clinical and laboratory
461 isolates of herpes simplex virus 1 reveals new mutations. J Virol 84:5303–13.

462 8. Kolb AW, Adams M, Cabot EL, Craven M, Brandt CR. 2011. Multiplex sequencing of seven
463 ocular herpes simplex virus type-1 genomes: phylogeny, sequence variability, and SNP
464 distribution. Invest Ophthalmol Vis Sci 52:9061–73.

465 9. Szpara ML, Gatherer D, Ochoa A, Greenbaum B, Dolan A, Bowden RJ, Enquist LW,
466 Legendre M, Davison AJ. 2014. Evolution and diversity in human herpes simplex virus
467 genomes. J Virol 88:1209–27.

468 10. Parsons LR, Tafuri YR, Shreve JT, Bowen CD, Shipley MM, Enquist LW, Szpara ML.
469 2015. Rapid genome assembly and comparison decode intrastrain variation in human
470 alphaherpesviruses. mBio 6:e02213-14.

471 11. Bowen CD, Renner DW, Shreve JT, Tafuri Y, Payne KM, Dix RD, Kinchington PR,
472 Gatherer D, Szpara ML. 2016. Viral forensic genomics reveals the relatedness of classic
473 herpes simplex virus strains KOS, KOS63, and KOS79. Virology 492:179–186.

474 12. Pfaff F, Groth M, Sauerbrei A, Zell R. 2016. Genotyping of herpes simplex virus type 1
475 (HSV-1) by whole genome sequencing. J Gen Virol.

476 13. Greninger AL, Roychoudhury P, Xie H, Casto A, Cent A, Pepper G, Koelle DM, Huang M-
477 L, Wald A, Johnston C, Jerome KR. 2018. Ultrasensitive Capture of Human Herpes
478 Simplex Virus Genomes Directly from Clinical Samples Reveals Extraordinarily Limited
479 Evolution in Cell Culture 3:12.

480 14. Davison AJ. 2012. Evolution of sexually transmitted and sexually transmissible human
481 herpesviruses. Ann N Y Acad Sci 1230:E37–E49.

482 15. Roizman B, Knipe DM, Whitley R. 2013. Herpes Simplex Viruses, p. 1823–1897. *In* Fields
483 Virology, 6th ed. Lippincott Williams & Wilkins, Philadelphia, PA.

484 16. Norberg P, Bergstrom T, Rekabdar E, Lindh M. 2004. Phylogenetic Analysis of Clinical
485 Herpes Simplex Virus Type 1 Isolates Identified Three Genetic Groups and Recombinant
486 Viruses. J Virol 78:10755–10764.

487 17. Norberg P. 2010. Divergence and genotyping of human alpha-herpesviruses: an overview.
488 Infect Genet Evol J Mol Epidemiol Evol Genet Infect Dis 10:14–25.

489 18. Kolb AW, Ané C, Brandt CR. 2013. Using HSV-1 genome phylogenetics to track past
490 human migrations. PloS One 8:1–9.

491 19. Sijmons S, Thys K, Mbong Ngwese M, Van Damme E, Dvorak J, Van Loock M, Li G,
492 Tachezy R, Busson L, Aerssens J, Van Ranst M, Maes P. 2015. High-Throughput Analysis
493 of Human Cytomegalovirus Genome Diversity Highlights the Widespread Occurrence of
494 Gene-Disrupting Mutations and Pervasive Recombination. J Virol 89:7673–7695.

495 20. Newman RM, Lamers SL, Weiner B, Ray SC, Colgrove RC, Diaz F, Jing L, Wang K, Saif S,
496 Young S, Henn M, Laeyendecker O, Tobian AAR, Cohen JI, Koelle DM, Quinn TC, Knipe
497 DM. 2015. Genome Sequencing and Analysis of Geographically Diverse Clinical Isolates
498 of Herpes Simplex Virus 2. J Virol JVI.01303-15.

499 21. Kolb AW, Larsen IV, Cuellar JA, Brandt CR. 2015. Genomic, Phylogenetic, and
500 Recombinational Characterization of Herpes Simplex Virus 2 Strains. J Virol 89:6427–
501 6434.

502 22. Tyler SD, Peters GA, Grose C, Severini A, Gray MJ, Upton C, Tipples GA. 2007. Genomic
503 cartography of varicella-zoster virus: a complete genome-based analysis of strain variability
504 with implications for attenuation and phenotypic differences. Virology 359:447–58.

505 23. Zell R, Taudien S, Pfaff F, Wutzler P, Platzer M, Sauerbrei A. 2012. Sequencing of 21
506 Varicella-Zoster Virus Genomes Reveals Two Novel Genotypes and Evidence of
507 Recombination. J Virol 86:1608–1622.

508 24. Depledge DP, Gray ER, Kundu S, Cooray S, Poulsen A, Aaby P, Breuer J. 2014. Evolution
509 of Cocirculating Varicella-Zoster Virus Genotypes during a Chickenpox Outbreak in
510 Guinea-Bissau. J Virol 88:13936–13946.

511 25. Kittles RA, Perola M, Peltonen L, Bergen AW, Aragon RA, Virkkunen M, Linnoila M,
512 Goldman D, Long JC. 1998. Dual Origins of Finns Revealed by Y Chromosome Haplotype
513 Variation. Am J Hum Genet 62:1171–1179.

514 26. Varilo T, Paunio T, Parker A, Perola M, Meyer J, Terwilliger JD, Peltonen L. 2003. The
515 interval of linkage disequilibrium (LD) detected with microsatellite and SNP markers in
516 chromosomes of Finnish populations with different histories. Hum Mol Genet 12:51–59.

517 27. Lappalainen T, Laitinen V, Salmela E, Andersen P, Huoponen K, Savontaus M-L, Lahermo
518 P. 2008. Migration Waves to the Baltic Sea Region. Ann Hum Genet 72:337–348.

519 28. Hannelius U, Salmela E, Lappalainen T, Guillot G, Lindgren CM, von Döbeln U, Lahermo
520 P, Kere J. 2008. Population substructure in Finland and Sweden revealed by the use of
521 spatial coordinates and a small number of unlinked autosomal SNPs. BMC Genet 9:54.

522 29. Ilonen J, Reijonen H, Green A, Reunanen A, Knip M, Simell O, Akerblom HK. 2000.
523 Geographical differences within Finland in the frequency of HLA-DQ genotypes associated
524 with type 1 diabetes susceptibility. The Childhood Diabetes in Finland Study Group. Eur J
525 Immunogenetics Off J Br Soc Histocompat Immunogenetics 27:225–230.

526 30. Paavilainen H, Lehtinen J, Romanovskaya A, Nygårdas M, Bamford DH, Poranen MM,
527 Hukkanen V. 2016. Inhibition of clinical pathogenic herpes simplex virus 1 strains with
528 enzymatically created siRNA pools: siRNA Pools Against Clinical HSV Strains. J Med
529 Virol 88:2196–2205.

530 31. Ziegler T, Waris M, Rautiainen M, Arstila P. 1988. Herpes simplex virus detection by
531 macroscopic reading after overnight incubation and immunoperoxidase staining. J Clin
532 Microbiol 26:2013–2017.

533 32. Hukkanen V, Rehn T, Kajander R, Sjöroos M, Waris M. 2000. Time-resolved fluorometry
534 PCR assay for rapid detection of herpes simplex virus in cerebrospinal fluid. J Clin
535 Microbiol 38:3214–3218.

536 33. Romanovskaya A, Paavilainen H, Nygårdas M, Bamford DH, Hukkanen V, Poranen MM.
537 2012. Enzymatically produced pools of canonical and Dicer-substrate siRNA molecules
538 display comparable gene silencing and antiviral activities against herpes simplex virus.
539 PloS One 7:e51019.

540 34. Szpara ML, Tafuri YR, Enquist LW. 2011. Preparation of viral DNA from nucleocapsids. J
541 Vis Exp JoVE 2–7.

542 35. Boukamp P, Petrussevska RT, Breitkreutz D, Hornung J, Markham A, Fusenig NE. 1988.
543 Normal keratinization in a spontaneously immortalized aneuploid human keratinocyte cell
544 line. J Cell Biol 106:761–771.

545 36. Post LE, Mackem S, Roizman B. 1981. Regulation of alpha genes of herpes simplex virus:
546 expression of chimeric genes produced by fusion of thymidine kinase with alpha gene
547 promoters. Cell 24:555–565.

548 37. Tardif KD, Jorgensen S, Langer J, Prichard M, Schlaberg R. 2014. Simultaneous titration
549 and phenotypic antiviral drug susceptibility testing for herpes simplex virus 1 and 2. J Clin
550 Virol 61:382–386.

551 38. Koboldt DC, Zhang Q, Larson DE, Shen D, McLellan MD, Lin L, Miller CA, Mardis ER,
552 Ding L, Wilson RK. 2012. VarScan 2: Somatic mutation and copy number alteration
553 discovery in cancer by exome sequencing. Genome Res 22:568–576.

554 39. Pandey U, Renner DW, Thompson RL, Szpara ML, Sawtell NM. 2017. Inferred father-to-
555 son transmission of herpes simplex virus results in near-perfect preservation of viral
556 genome identity and in vivo phenotypes. Sci Rep 7:13666.

557 40. Nakamura K, Oshima T, Morimoto T, Ikeda S, Yoshikawa H, Shiwa Y, Ishikawa S, Linak
558 MC, Hirai A, Takahashi H, Altaf-Ul-Amin M, Ogasawara N, Kanaya S. 2011. Sequence-
559 specific error profile of Illumina sequencers. Nucleic Acids Res 39:1–13.

560 41. Depledge DP, Kundu S, Jensen NJ, Gray ER, Jones M, Steinberg S, Gershon A, Kinchington
561 PR, Schmid DS, Balloux F, Nichols RA, Breuer J. 2014. Deep Sequencing of Viral
562 Genomes Provides Insight into the Evolution and Pathogenesis of Varicella Zoster Virus
563 and Its Vaccine in Humans. Mol Biol Evol 31:397–409.

564 42. Cingolani P, Platts A, Wang LL, Coon M, Nguyen T, Wang L, Land SJ, Lu X, Ruden DM.
565 2012. A program for annotating and predicting the effects of single nucleotide
566 polymorphisms, SnpEff. Fly (Austin) 6:80–92.

567 43. Cingolani P, Patel VM, Coon M, Nguyen T, Land SJ, Ruden DM, Lu X. 2012. Using
568 Drosophila melanogaster as a Model for Genotoxic Chemical Mutational Studies with a
569 New Program, SnpSift. Front Genet 3.

570 44. Igarashi K, Fawl R, Roller RJ, Roizman B. 1993. Construction and properties of a
571 recombinant herpes simplex virus 1 lacking both S-component origins of DNA synthesis. J
572 Virol 67:2123–2132.

573 45. Norberg P, Olofsson S, Tarp MA, Clausen H, Bergstrom T, Liljeqvist JA. 2007.
574 Glycoprotein I of herpes simplex virus type 1 contains a unique polymorphic tandem-
575 repeated mucin region. J Gen Virol 88:1683–1688.

576 46. Reynolds AE, Wills EG, Roller RJ, Ryckman BJ, Baines JD. 2002. Ultrastructural
577 localization of the herpes simplex virus type 1 UL31, UL34, and US3 proteins suggests
578 specific roles in primary envelopment and egress of nucleocapsids. J Virol 76:8939–52.

579 47. Roller RJ, Bjerke SL, Haugo AC, Hanson S. 2010. Analysis of a Charge Cluster Mutation of
580 Herpes Simplex Virus Type 1 UL34 and Its Extragenic Suppressor Suggests a Novel

581 Interaction between pUL34 and pUL31 That Is Necessary for Membrane Curvature around
582 Capsids. J Virol 84:3921–3934.

583 48. Buchman TG, Simpson T, Nosal C, Roizman B. 1980. The Stucture of Herpes Simplex Virus
584 DNA and its Application to Molecular Epidemiology. Ann N Y Acad Sci 354:279–290.

585 49. Rastrojo A, López-Muñoz AD, Alcamí A. 2017. Genome Sequence of Herpes Simplex Virus
586 1 Strain SC16. Genome Announc 5:e01392-16.

587 50. Skoblov MY, Lavrov AV, Bragin AG, Zubtsov DA, Andronova VL, Galegov GA, Skoblov
588 YS. 2017. The genome nucleotide sequence of herpes simplex virus 1 strain L2. Russ J
589 Bioorganic Chem 43:140–142.

590 51. Petro CD, Weinrick B, Khajoueinejad N, Burn C, Sellers R, Jacobs WR, Herold BC. 2016.
591 HSV-2 ΔgD elicits FcγR-effector antibodies that protect against clinical isolates. JCI
592 Insight 1.

593 52. Lee K, Kolb AW, Sverchkov Y, Cuellar JA, Craven M, Brandt CR. 2015. Recombination
594 Analysis of Herpes Simplex Virus 1 Reveals a Bias toward GC Content and the Inverted
595 Repeat Regions. J Virol 89:7214–7223.

596 53. Bondre VP, Sankararaman V, Andhare V, Tupekar M, Sapkal GN. 2016. Genetic
597 characterization of human herpesvirus type 1: Full-length genome sequence of strain
598 obtained from an encephalitis case from India. Indian J Med Res 144:750–760.

599 54. Parsons LR, Tafuri YR, Shreve JT, Bowen CD, Shipley MM, Enquist LW, Szpara ML.
600 2015. Rapid Genome Assembly and Comparison Decode Intrastrain Variation in Human
601 Alphaherpesviruses. mBio 6:e02213-14.

602 55. Norberg P, Tyler S, Severini A, Whitley R, Liljeqvist J-A, Bergstrom T. 2011. A genome-
603 wide comparative evolutionary analysis of herpes simplex virus type 1 and varicella zoster
604 virus. PloS One 6:1–8.

605

606 # Tables

607 **Table 1: The Finnish HSV-1 strains used for genome sequence comparisons.**

Sample	Gender	Code	Age	Lesion or diagnosis	Acyclovir sensitivity, IC50 value (µg/ml)
H1211	female	F-11	21	blister	0.25
H1215	male	M-15	5	blister	0.03
H12113	female	F-13	29	blister	0.11
H12114	female	F-14g	23	genital blister	0.50
H12117	female	F-17	57	blister	0.15
H12118	female	F-18g	19	genital blister	0.13
H1311	female	F-11*l*	59	blister (lip)	0.31
H1312	male	M-12	39	blister	0.13
H1412	female	F-12g	28	genital lesion	0.09
H15119	male	M-19	36	blister	0.15

608 *The IC50 value for HSV-1 delta305 (a TK-negative, ACV-resistant, positive-control) was 8.08
609 and for the reference strain HSV-1(17+) it was 0.13. The limit of resistance was ≥2.0 µg/ml.

610

611 **Table 2. Sequencing statistics for Finnish HSV-1 strains.**

Sample	Code	% Depth ≥100	Average coverage	Raw Sequence Reads	Used for Assembly	% Viral	GenBank Accession^
H1211	F-11	96%	1,027x	4.2 million	2.8 million	66%	MH999843
H1215	M-15	99%	2,808x	5.5 million	3.8 million	70%	MH999846
H12113	F-13	98%	2,354x	3.8 million	2.4 million	64%	MH999842
H12114	F-14g	98%	2,078x	5.9 million	3.8 million	66%	MH999844
H12117	F-17	98%	1,976x	4.1 million	2.7 million	66%	MH999845
H12118	F-18g	98%	1,678x	4.2 million	2.9 million	69%	MH999847
H1311	F-11*l*	99%	2,541x	4.6 million	3.0 million	65%	MH999848
H1312	M-12	98%	2,415x	6.0 million	3.7 million	61%	MH999849
H1412	F-12g	98%	1,524x	4.5 million	3.1 million	69%	MH999851
H15119	M-19	99%	1,536x	4.8 million	3.0 million	64%	MH999850

612 ^See GenBank flatfile attached for review purposes.

613

614 # Figures & Figure Legends

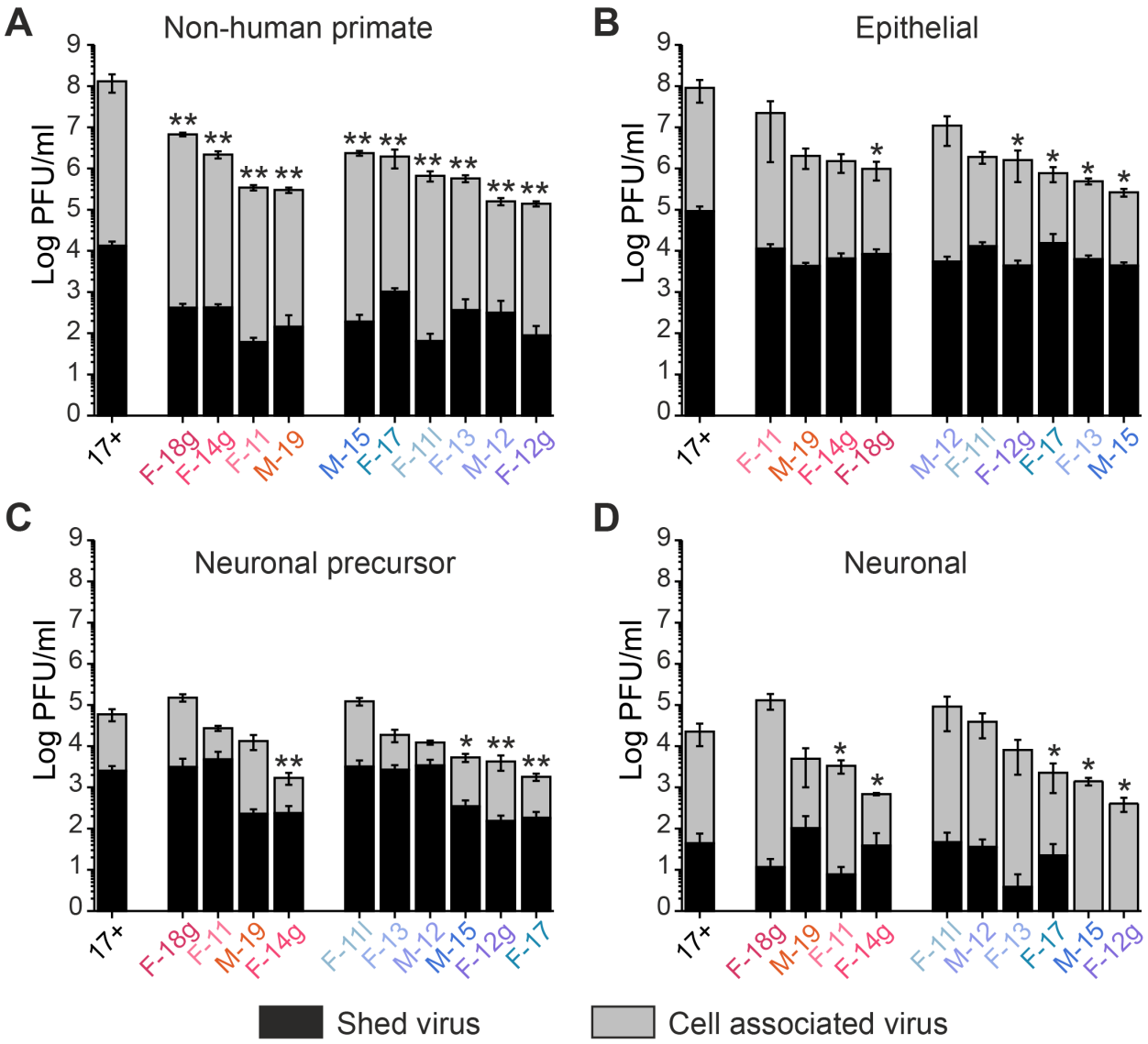

615

616 **Figure 1: Comparison of growth properties of Finnish HSV-1 strains reveals the**

617 **uncoupling of phenotypic and geographic variation.**

618 Histograms comparing virus production for ten Finnish strains of HSV-1, as compared to the

619 HSV-1 reference strain 17+, in different cell types. Panel **(A,** non-human primate**)** shows Vero

620 monkey kidney cells, which are defective in interferon signaling; **(B)** shows HaCaT human
621 epithelial cells; **(C)** shows undifferentiated human SH-SY5Y neuroblastoma cells (neuronal
622 precursor cells); **(D)** shows differentiated human SH-SY5Y neuronal-like cells. Viruses are
623 plotted in descending order based on their viral production, and divided into their genomic sub-
624 groups (see **Figure 4**). Each histogram bar plots infectious virions in the cell-associated fraction
625 (gray) vs. those released from cells (black). **Supplemental Figure S1** shows the same data, but
626 with extracellular released virus plotted as a percentage of total virus production. Bar shows
627 SEM; * = p=<0.05, ** = p<0.001 as compared to the total virus amount (cell associated + shed),
628 clinical isolate vs HSV-1(17+) reference strain.

629

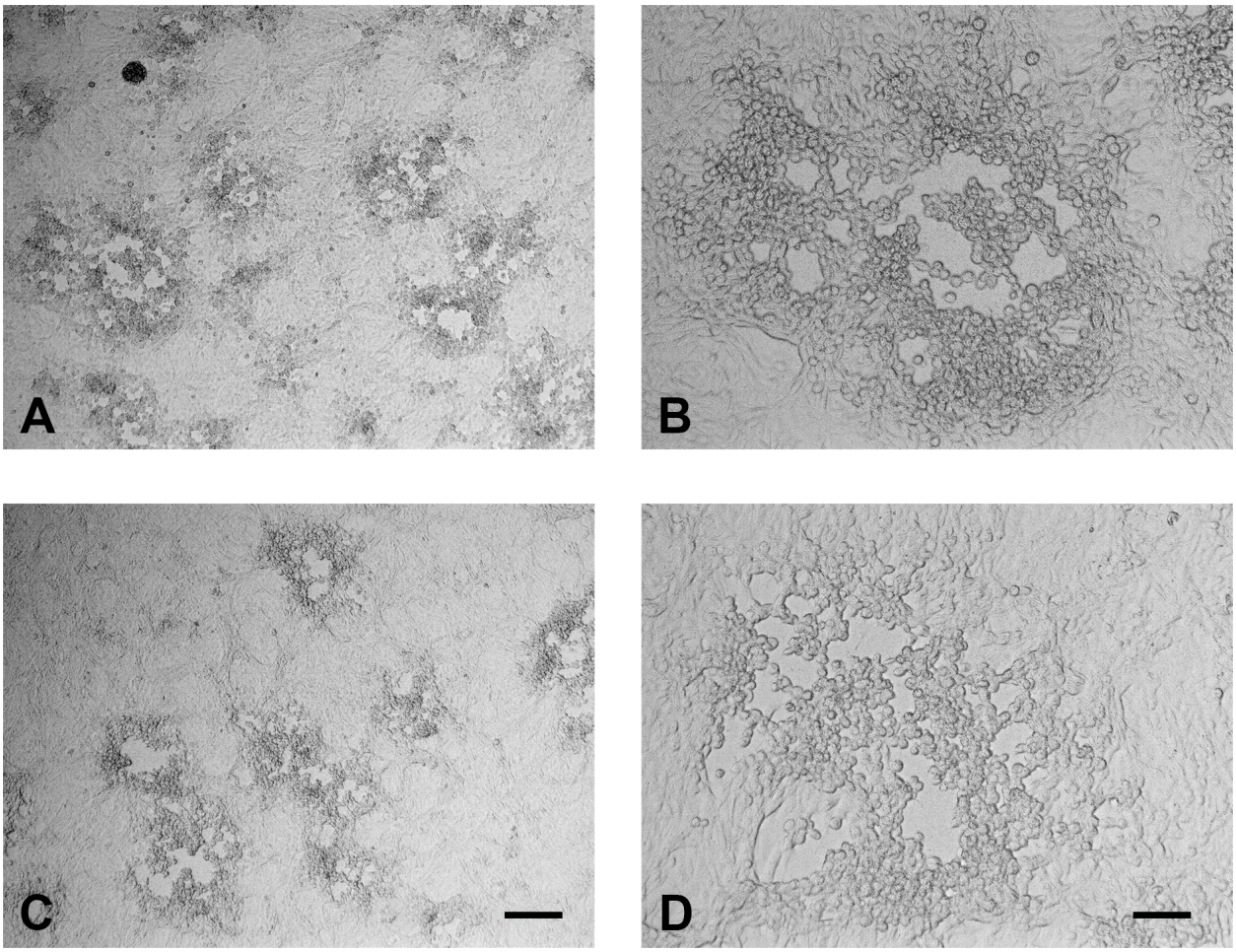

Figure 2. Finnish HSV-1 strains have similar plaque morphology.

Typical morphology of the plaques of the clinical HSV-1 isolates on Vero cells, at 48 hours post infection. Plaques are shown at low magnification (4X, **A,C**), as well as high magnification (10X, **B,D**). Isolates M-19 (**A-B**) and F-12g (**C,D**) serve as representative examples. These two isolates also represent the two sub-groups of Finnish HSV-1 isolates detected in **Figures 3-4**, as well as samples annotated as blister-derived (M-19) and genital-blister-derived (F-12g) (see also **Table 1**). The scale bar corresponds to 100 μm in panels A and C, and to 50 μm in panels B and D.

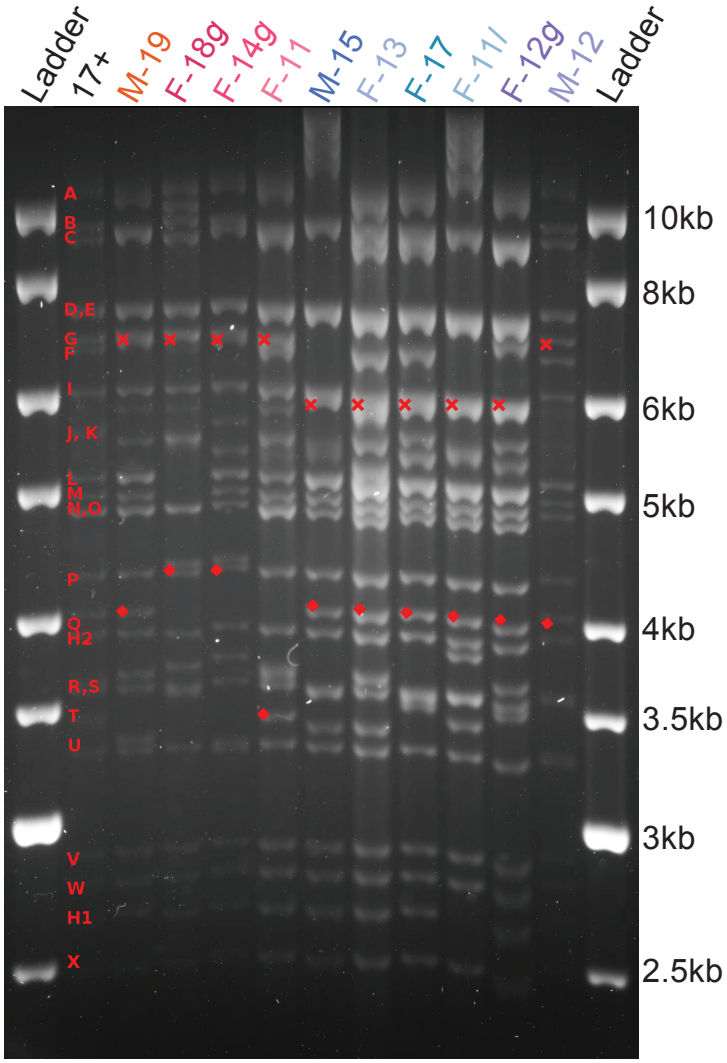

Figure 3: RFLP comparison reveals at least two sub-groups of Finnish HSV-1 strains.

Viral genomic DNA was digested with SalI and separated via electrophoresis to distinguish overall genetic patterns. Classically defined SalI fragment notations (red alphabet letters) are indicated on the left (48). Predicted SalI cut-sites in each viral genome are shown in **Supplemental Figure S2**. Red crosses (x) indicate variation in the size of SalI fragment G, while diamonds indicate variation in the SalI Q fragment.

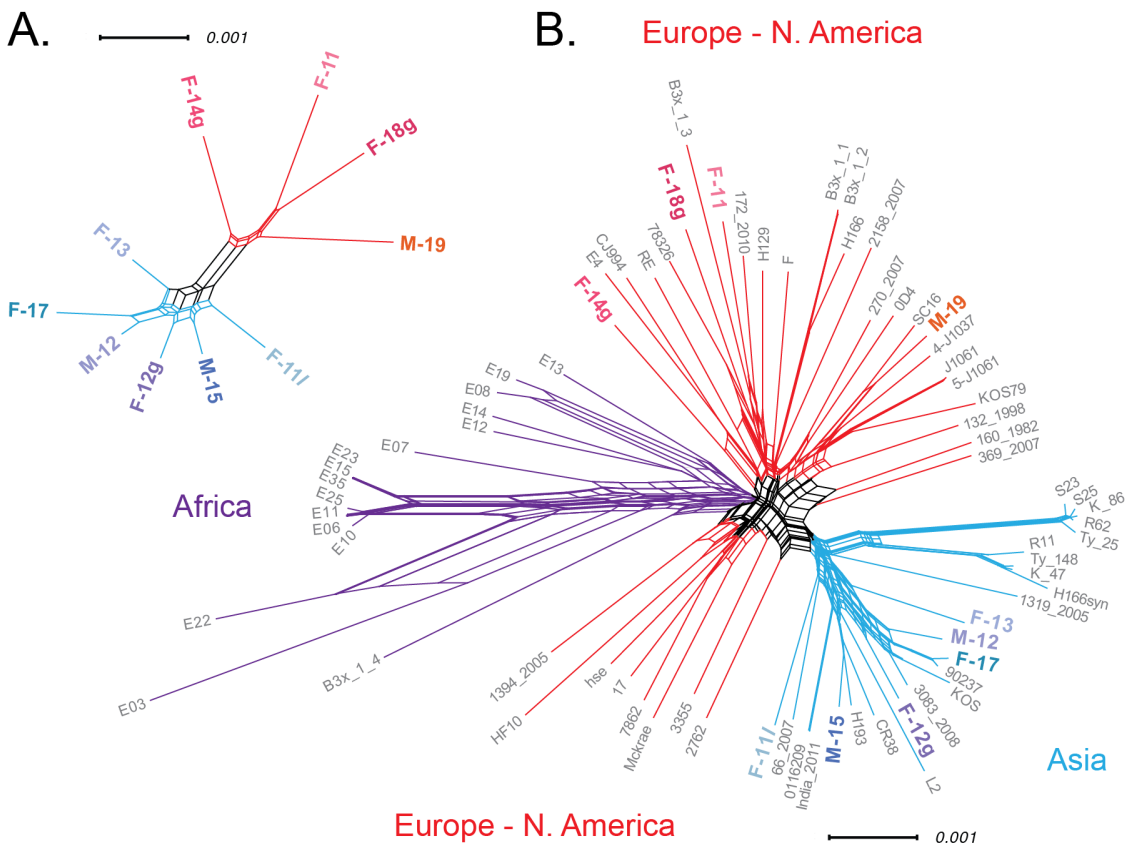

647

648 **Figure 4. A network graph of genetic relatedness reveals that Finland HSV-1**

649 **isolates separate into two sub-groups.**

650 A network graph of genetic relatedness was constructed using SplitsTree4 to demonstrate how

651 the ten new Finland HSV-1 isolates relate to each other (**A**) and to previously described HSV-1

652 genomes from a diversity of locations (**B**). Geographic clustering of branches and clades

653 resemble those previously described (9, 16–18) and are colored by origin of strains: red for

654 Europe and North America, blue for Asia, and purple for Africa. Finland HSV-1 genomes are

655 indicated in bold, and separate into two sub-groups (**A**), which appear to relate previously

656 recognized Asian and European and North American clades. The isolate name, country of origin,

657 GenBank accession, and reference(s) for each previously described HSV-1 genome are listed in

658 **Supplemental Table S1**.

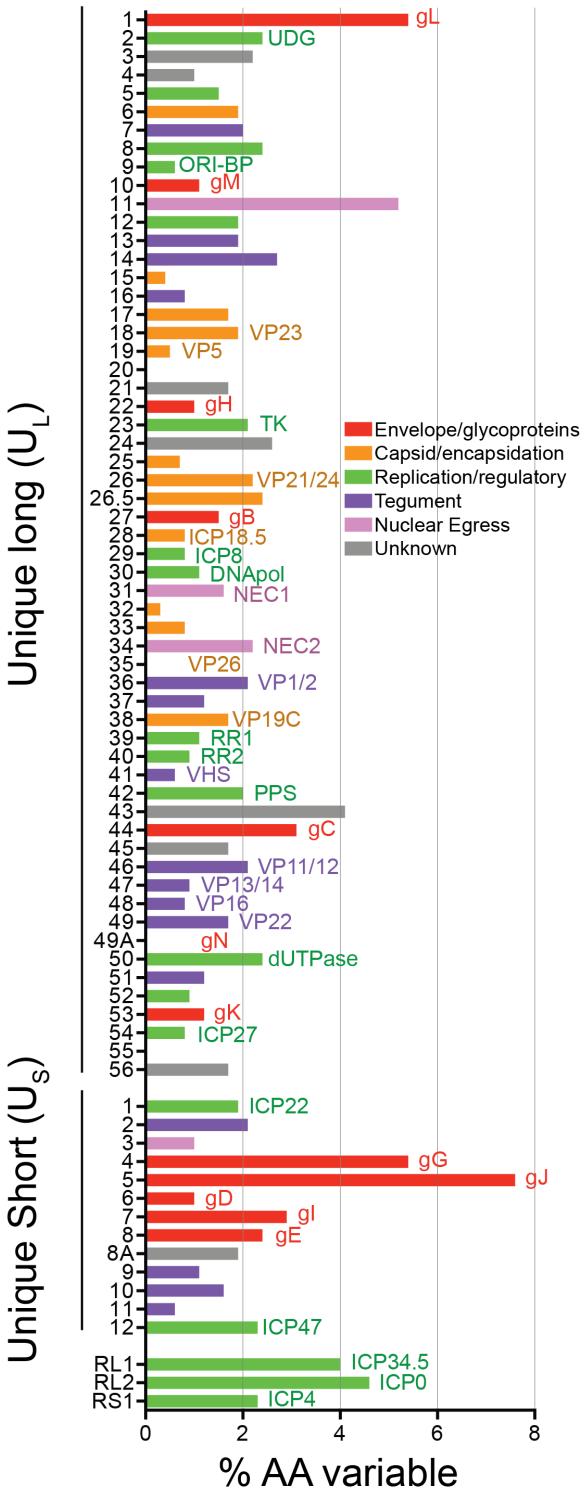

Figure 5. Substantial protein-coding variation exists between Finland HSV-1 isolates.

662 Histogram showing each protein of the HSV-1 genome and its percent amino acid (AA) variation
663 between the ten Finnish HSV-1 strains compared here. Labels for the Unique Long (UL) and
664 Unique Short (US) regions of the HSV-1 genome are shown in summary format, to the left of
665 each sequentially-numbered viral coding region. Where possible, the common name of each
666 protein is shown to the right of the appropriate histogram bar, e.g. UL1 is also known as gL. AA
667 differences were quantified at the consensus level of each viral genome. See **Supplemental**
668 **Table S2** for additional data on the number of nucleotide differences and dN/dS ratio for each
669 gene.

670

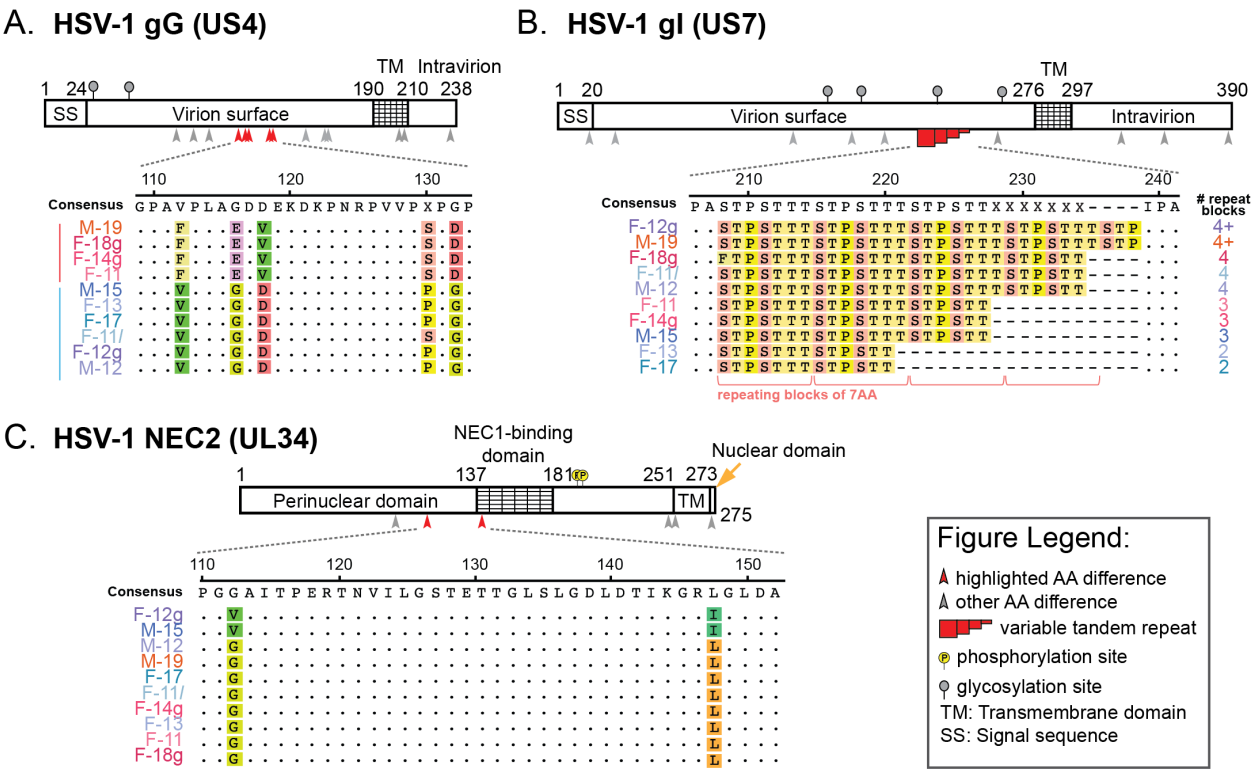

Figure 6. Patterns of genetic variation in Finnish HSV-1 strains correlate with genomic and phenotypic data.

Diagrams depict three HSV-1 proteins with known functional domains and post-translational modifications (e.g. phosphorylation, glycosylation; see Legend). A subset of each protein is highlighted via an AA alignment of the ten clinical HSV-1 isolates. (**A**) Coding differences in the secreted and virion surface glycoprotein G (gG; US4) correlate with the overall genomic sub-groups (clades) shown in **Figure 4**. (**B**) Variation in copy number of a seven AA tandem repeat block in glycoprotein I (gI; US7) changes the length of a repeating tract of mucin-type O-linked glycosylation sites, as described previously in clinical isolates of HSV-1 (16, 45). (**C**) AA differences in the nuclear egress protein NEC2 (UL34) were observed in the two strains (M-15, F-12g) which showed no detectable extracellular virion release in differentiated neuronal cells (**Figure 1D**).

685 # Supplementary Table & Figures

686 **Supplemental Table S1: List of previously published HSV-1 genomes used for**

687 **phylogenetic analyses**

Virus Isolate	Country (with location detail, if available)	GenBank Accession #	References
H1211 / F-11*	Finland	MH999843	(30), present
H1215 / M-15*	Finland	MH999846	(30), present
H12113 / F-13*	Finland	MH999842	present
H12114 / F-14g*	Finland	MH999844	(30), present
H12117 / F-17*	Finland	MH999845	(30), present
H12118 / F-18g*	Finland	MH999847	(30), present
H1311 / F11*l*	Finland	MH999848	present
H1312 / M-12*	Finland	MH999849	present
H1412 / F-12g*	Finland	MH999851	present
H15119 / M-19*	Finland	MH999850	present
SC16	Spain (Madrid)	KX946970	(49)
172/2010	Germany	LT594105	(12)
2158/2007	Germany	LT594106	(12)
3083/2008	Germany	LT594107	(12)
1319/2005	Germany	LT594108	(12)
270/2007	Germany	LT594109	(12)
66/2007	Germany	LT594110	(12)
1394/2005	Germany	LT594111	(12)
369/2007	Germany	LT594112	(12)
160/1982	Germany	LT594192	(12)
132/1998	Germany	LT594457	(12)
L2	Russia (Moscow)	KT780616	(50)
B^3x1.1	U.S.A. (Bronx, NY)	KU310657	(51)
B^3x1.2	U.S.A. (Bronx, NY)	KU310658	(51)
B^3x1.3	U.S.A. (Bronx, NY)	KU310659	(51)
B^3x1.4	U.S.A. (Bronx, NY)	KU310660	(51)
B^3x1.5	U.S.A. (Bronx, NY)	KU310661	(51)
H193	U.S.A.	KT425108	n/a
KOS79	U.S.A. (Madison, WI)	KT425109	(11)
CJ994	U.S.A. (Madison, WI)	KR011283	(52)
HSV-1/0116209/India/2011	India	KJ847330	(53)
H166	U.S.A.	KM222726	(54)
H166syn	U.S.A.	KM222727	(54)
RE	U.S.A.	KF498959	n/a
OD4	U.S.A. (Madison, WI)	JN420342	(8)
17	U.K. (Glasgow)	JN555585	(9)
CR38	China (Shenyang)	HM585508	(9)

Virus Isolate	Country (with location detail, if available)	GenBank Accession #	References
E03	Kenya (Nairobi)	HM585509	(9)
E06	Kenya (Nairobi)	HM585496	(9)
E07	Kenya (Nairobi)	HM585497	(9)
E08	Kenya (Nairobi)	HM585498	(9)
E10	Kenya (Nairobi)	HM585499	(9)
E11	Kenya (Nairobi)	HM585500	(9)
E12	Kenya (Nairobi)	HM585501	(9)
E13	Kenya (Nairobi)	HM585502	(9)
E14	Kenya (Nairobi)	HM585510	(9)
E15	Kenya (Nairobi)	HM585503	(9)
E19	Kenya (Nairobi)	HM585511	(9)
E22	Kenya (Nairobi)	HM585504	(9)
E23	Kenya (Nairobi)	HM585505	(9)
E25	Kenya (Nairobi)	HM585506	(9)
E35	Kenya (Nairobi)	HM585507	(9)
R11	South Korea (Seoul)	HM585514	(9)
R62	South Korea (Seoul)	HM585515	(9)
S23	Japan (Sapporo)	HM585512	(9)
S25	Japan (Sapporo)	HM585513	(9)
F	U.S.A. (Chicago, IL)	GU734771	(9)
H129	U.S.A. (San Francisco, CA)	GU734772	(9)
McKrae	U.S.A. (Gainesville, FL)	JQ730035, JX142173	(9)
KOS	U.S.A. (Houston, TX)	JQ673480, JQ780693	(9)
HF10	U.S.A. (New York, NY)	DQ889502	(9)
Ty_25	Japan	MH999840	n/a
Ty_148	Japan	MH999841	n/a
K_86	Japan	MH999839	n/a
K_47	Japan	MH999838	n/a
7-hse †	Sweden or U.S.A.	SRX056767	(55)
7862 †	Sweden or U.S.A.	SRX056770	(55)
3355 †	Sweden or U.S.A.	SRX056769	(55)
2762 †	Sweden or U.S.A.	SRX056768	(55)
90237 †	Sweden or U.S.A.	SRX056772	(55)
E4 †	Sweden or U.S.A.	SRX056773	(55)
78326 †	Sweden or U.S.A.	SRX056771	(55)
4-J1037 †	Sweden or U.S.A.	SRX056760	(55)
J1061 †	Sweden or U.S.A.	SRX056774	(55)
5-J1061	Sweden or U.S.A.	n/a	(55)

688 * newly sequenced strains from Finland in this study.

689 † Sequence data deposited in GenBank short read archive

690

691 **Supplemental Table S2: Number of nucleotide and amino acid (AA) differences observed in each set of Finnish or**

692 **worldwide published HSV1 genomes.**

Gene*	ORF length in NT^	protein length (#AA)	10 Finnish # NT diff.^	10 Finnish # AA changes	10 Finnish %AA diff.	10 Finnish dN/dS	All HSV1 # NT diff.	All HSV1 # AA changes	All HSV1 %AA diff.	All HSV1 dN/dS ratio
UL1	675	224	22	12	5.4	1.20	58	31	13.8	1.15
UL2	1005	334	24	8	2.4	0.50	62	28	8.4	0.82
UL3	675	224	13	5	2.2	0.63	43	19	8.5	0.79
UL4	600	199	11	2	1.0	0.22	43	18	9.0	0.72
UL5	2649	882	35	13	1.5	0.59	106	38	4.3	0.56
UL6	2031	676	43	13	1.9	0.43	107	30	4.4	0.39
UL7	891	296	24	6	2.0	0.33	47	17	5.7	0.57
UL8	2253	750	44	18	2.4	0.69	124	62	8.3	1.00
UL9	2556	851	21	5	0.6	0.31	110	32	3.8	0.41
UL10	1422	473	25	5	1.1	0.25	81	30	6.3	0.59
UL11	291	96	13	5	5.2	0.63	26	17	17.7	1.89
UL12	1881	626	36	12	1.9	0.50	87	30	4.8	0.53
UL13	1557	518	27	10	1.9	0.59	72	33	6.4	0.85
UL14	660	219	10	6	2.7	1.50	27	15	6.8	1.25
UL15	2208	735	22	3	0.4	0.16	80	16	2.2	0.25
UL16	1122	373	13	3	0.8	0.30	55	19	5.1	0.53
UL17	2112	703	30	12	1.7	0.67	108	39	5.5	0.57
UL18	957	318	12	6	1.9	1.00	41	15	4.7	0.58
UL19	4125	1374	39	7	0.5	0.22	139	40	2.9	0.40
UL20	669	222	7	0	0.0	0.00	29	9	4.1	0.45
UL21	1608	535	20	9	1.7	0.82	70	25	4.7	0.56
UL22	2517	838	21	8	1.0	0.62	120	50	6.0	0.71
UL23	1131	376	21	8	2.1	0.62	63	26	6.9	0.70
UL24	810	269	18	7	2.6	0.64	60	28	10.4	0.88

Gene*	ORF length in NT^	protein length (#AA)	10 Finnish # NT diff.^	10 Finnish # AA changes	10 Finnish %AA diff.	10 Finnish dN/dS	All HSV1 # NT diff.	All HSV1 # AA changes	All HSV1 %AA diff.	All HSV1 dN/dS ratio
UL25	1743	580	19	4	0.7	0.27	74	25	4.3	0.51
UL26	1908	635	40	14	2.2	0.54	92	34	5.4	0.59
UL26.5	990	329	21	8	2.4	0.62	45	17	5.2	0.61
UL27	2715	904	51	14	1.5	0.38	123	40	4.4	0.48
UL28	2358	785	26	6	0.8	0.30	87	23	2.9	0.36
UL29	3591	1196	54	10	0.8	0.23	154	33	2.8	0.27
UL30	3708	1235	32	13	1.1	0.68	154	49	4.0	0.47
UL31	921	306	15	5	1.6	0.50	34	13	4.2	0.62
UL32	1791	596	20	2	0.3	0.11	85	28	4.7	0.49
UL33	393	130	2	1	0.8	1.00	14	4	3.1	0.40
UL34	828	275	15	6	2.2	0.67	37	14	5.1	0.61
UL35	339	112	1	0	0.0	0.00	8	1	0.9	0.14
UL36	9420	3139	166	66	2.1	0.66	1271	440	14.0	0.53
UL37	3372	1123	41	13	1.2	0.46	140	60	5.3	0.75
UL38	1398	465	18	8	1.7	0.80	70	30	6.5	0.75
UL39	3414	1137	42	13	1.1	0.45	157	61	5.4	0.64
UL40	1023	340	10	3	0.9	0.43	38	12	3.5	0.46
UL41	1470	489	16	3	0.6	0.23	52	22	4.5	0.73
UL42	1467	488	19	10	2.0	1.11	76	39	8.0	1.05
UL43	1254	417	35	17	4.1	0.94	90	50	12.0	1.25
UL44	1536	511	26	16	3.1	1.60	97	55	10.8	1.31
UL45	519	172	4	3	1.7	3.00	22	8	4.7	0.57
UL46	2157	718	33	15	2.1	0.83	111	65	9.1	1.41
UL47	2082	693	29	6	0.9	0.26	81	29	4.2	0.56
UL48	1473	490	18	4	0.8	0.29	69	25	5.1	0.57
UL49	276	301	13	5	1.7	0.63	42	18	6.0	0.75
UL49A	906	91	2	0	0.0	0.00	8	3	3.3	0.60
UL50	1116	371	23	9	2.4	0.64	65	26	7.0	0.67

Gene*	ORF length in NT^	protein length (#AA)	10 Finnish # NT diff.^	10 Finnish # AA changes	10 Finnish %AA diff.	10 Finnish dN/dS	All HSV1 # NT diff.	All HSV1 # AA changes	All HSV1 %AA diff.	All HSV1 dN/dS ratio
UL51	735	244	12	3	1.2	0.33	33	13	5.3	0.65
UL52	3177	1058	43	9	0.9	0.26	129	41	3.9	0.47
UL53	1017	338	16	4	1.2	0.33	36	12	3.6	0.50
UL54	1539	512	11	4	0.8	0.57	73	34	6.6	0.87
UL55	561	186	5	0	0.0	0.00	25	9	4.8	0.56
UL56	705	234	8	4	1.7	1.00	34	19	8.1	1.27
US1	1263	420	22	8	1.9	0.57	75	39	9.3	1.08
US2	876	291	24	6	2.1	0.33	44	14	4.8	0.47
US3	1446	481	14	5	1.0	0.56	57	21	4.4	0.58
US4	717	238	26	13	5.5	1.00	68	36	15.1	1.13
US5	279	92	10	7	7.6	2.33	25	17	18.5	2.13
US6	1185	394	18	4	1.0	0.29	67	18	4.6	0.37
US7	1173	390	28	12	3.1	0.75	119	57	14.6	0.92
US8	1653	159	30	13	8.2	0.76	79	38	23.9	0.93
US8A	480	550	3	3	0.5	1.00	49	15	2.7	0.44
US9	273	90	1	1	1.1	1.00	12	4	4.4	0.50
US10	939	312	11	5	1.6	0.83	65	29	9.3	0.81
US11	486	161	1	1	0.6	1.00	42	19	11.8	0.83
US12	267	88	4	2	2.3	1.00	17	10	11.4	1.43
RL1	747	248	25	11	4.4	0.79	422	90	36.3	0.27
RL2	2328	775	44	20	2.6	0.83	180	91	11.7	1.02
RS1	3897	1298	62	30	2.3	0.94	345	207	15.9	1.50

693 * See **Supplemental Table S1** for list of strain names and genome accessions for comparisons of 10 Finnish and all published HSV1 genomes.
694 See **Supplemental Table S3** for list of strains excluded from selected gene alignments due to missing data in GenBank.
695 ^ Abbreviations: ORF, open reading frame; NT, nucleotide; AA, amino acid; diff., difference; %, percent; dN/dS, ratio of nonsynonymous to
696 synonymous nucleotide changes

697 **Supplemental Table S3: HSV-1 strains used to calculate nucleotide and amino acid**

698 **(AA) differences in Supplemental Table S2 and Figure 5.**

Gene	# of strains in nucleotide alignment	# of strains in AA alignment	Strains not used in nucleotide and AA alignments*
UL7	60	60	B^3x1.1, B^3x1.2, B^3x1.3, B^3x1.4, B^3x1.5
UL12	61	61	B^3x1.3, B^3x1.4, B^3x1.5, RE
UL13	58	58	E06, E25, E11, OD4, B^3x1.3, B^3x1.4, B^3x1.5
UL15	60	60	B^3x1.1, B^3x1.2, B^3x1.3, B^3x1.4, B^3x1.5
UL19	61	61	B^3x1.3, B^3x1.4, B^3x1.5, RE
UL26.5	61	61	B^3x1.3, B^3x1.4, B^3x1.5, HF10
UL41	61	61	B^3x1.3, B^3x1.4, B^3x1.5, OD4
UL43	61	61	B^3x1.3, B^3x1.4, B^3x1.5, HF10
UL48	60	60	B^3x1.1, B^3x1.2, B^3x1.3, B^3x1.4, B^3x1.5
UL49A	51	51	B^3x1.3, B^3x1.4, B^3x1.5, HF10, 66_2007, 369_2007, 160_1982, 1394_2005, 132_1998, 3083_2008, 2158_2007, 172_2010, 270_2007, 1319_2005
UL55	59	59	E35, E13, KUTy25, B^3x1.3, B^3x1.4, B^3x1.5
UL56	60	60	B^3x1.3, B^3x1.4, B^3x1.5, E35, HF10
US1	60	60	B^3x1.1, B^3x1.2, B^3x1.3, B^3x1.4, B^3x1.5
US8A	61	61	HF10, B^3x1.3, B^3x1.4, B^3x1.5
RL1	58	58	B^3x1.3, B^3x1.4, B^3x1.5, OD4, 1394_2005, CJ994, L2
RL2	61	61	B^3x1.3, B^3x1.4, B^3x1.5, B^3x1.2
RS1	59	59	B^3x1.3, B^3x1.4, B^3x1.5, S23, CJ994, L2
All other genes	62	62	B^3x1.3, B^3x1.4, B^3x1.5

699 * Strains were excluded due to missing data (e.g. due to sequencing gaps) or annotations in
700 GenBank.
701

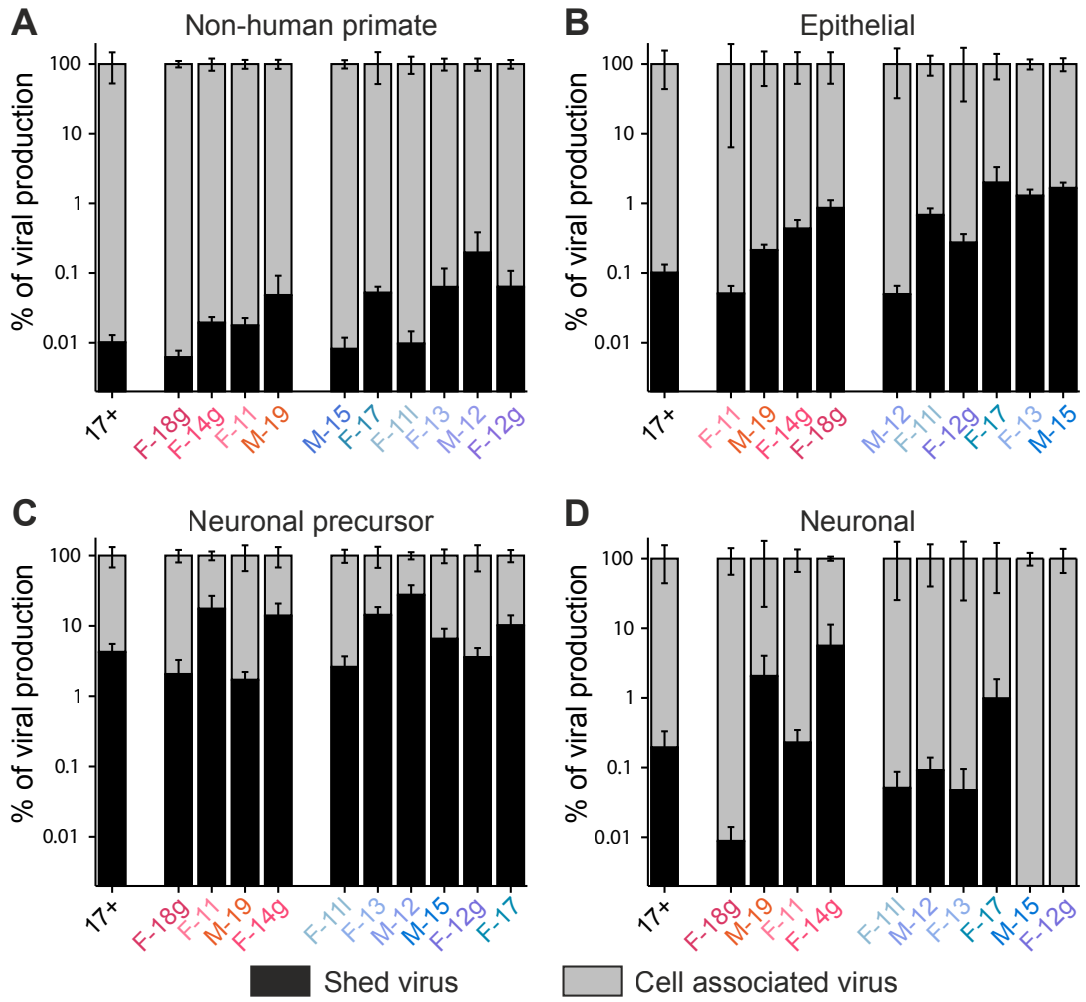

Supplemental Figure S1. Viral production as percent values in shed and cell-associated fractions.

Histograms compare virus production for ten Finnish strains of HSV-1, as compared to the HSV-1 reference strain 17+, in different cell types. These data are the same as those shown in **Figure 1**, but here extracellular released virus, or shed virus (black), is plotted as a percentage of total virus production (gray). Viruses are plotted in the same order as **Figure 1**, which is descending based on their viral production, within each genomic sub-group (see **Figure 4**). Panel (**A,** non-human primate) shows Vero monkey kidney cells, which are defective in interferon signaling;

711 **(B)** shows HaCaT human epithelial cells; **(C)** shows undifferentiated human SH-SY5Y
712 neuroblastoma cells (neuronal precursor cells); **(D)** shows differentiated human SH-SY5Y
713 neuronal-like cells. Bar shows SEM.

714

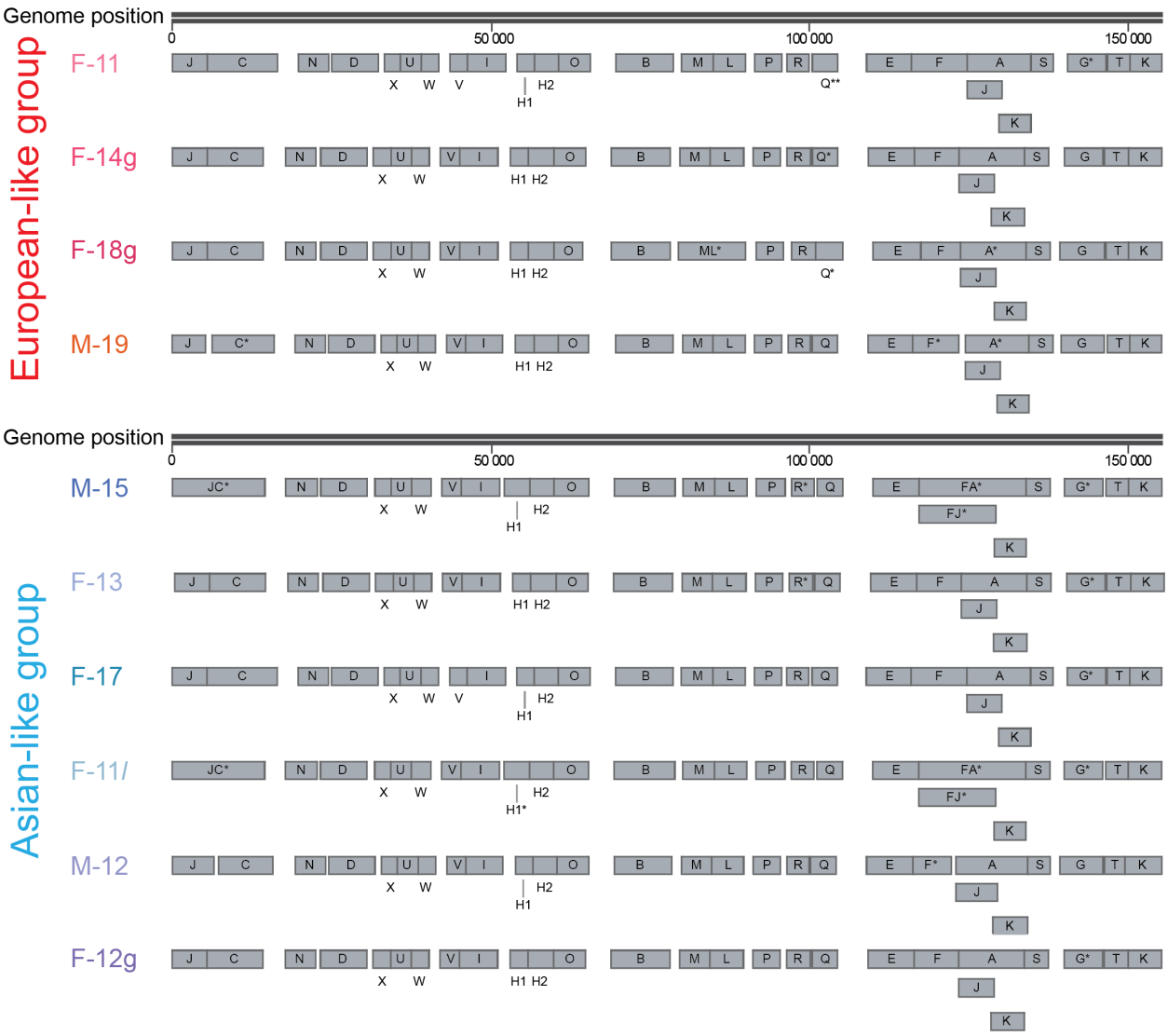

715

716 **Supplemental Figure S2: Diagrams depict the predicted SalI cut-sites in 10 Finnish**

717 **HSV-1 genomes.**

718 A computational prediction of SalI restriction sites is shown for each viral consensus genome.

719 Classically defined SalI fragment notations (alphabet letters) are indicated on each major

720 fragment. These maps were compared to the experimentally observed fragments in **Figure 3**.

721 Genomic sub-groups are as diagrammed in **Figure 4**.

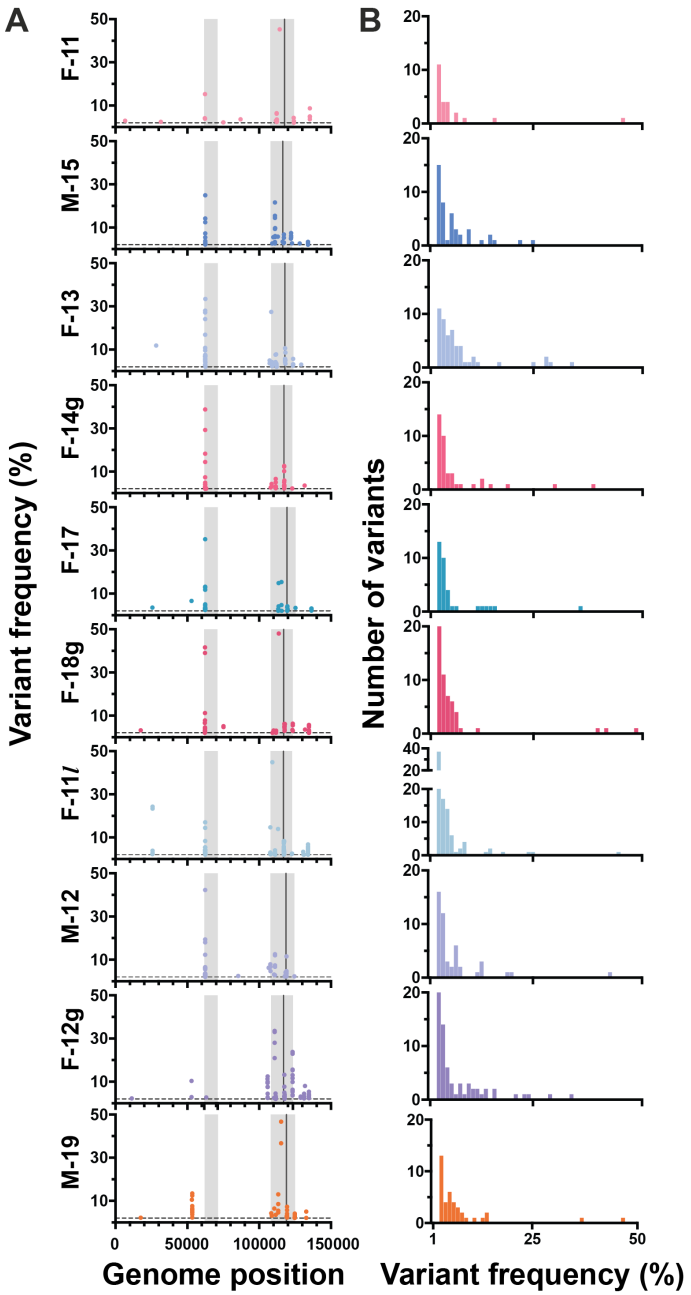

722

723 **Supplemental Figure S3. Scatter plots demonstrate the distribution of minority**

724 **variants in each Finnish HSV-1 genome.**

725 **(A)** Scatter plots demonstrate the position (x-axis) and frequency (y-axis) of minority variants

726 detected in each Finnish HSV-1 genome. The limit of detection was set at 2% (see Methods for

727 details). Stochastic aspects of alignment at tandem repeats can generate excess signals of

728 minority variants near these areas, as can be seen in VP1/2 (UL36) and in the internal-repeat
729 regions (areas denoted in gray on x-axis). **(B)** Histograms depict the total number of minority
730 variants (y-axis) in each frequency bin (x-axis) for each strain of Finnish HSV-1. Bins are in 1%
731 increments.

732